

°C). The structure of water in both solutions is different from that of bulk water; the peaks in the radial distribution curve of the solutions due to the second-nearest oxygen-oxygen interference are found at longer distances than that of bulk water, while those for the distance of the first-nearest neighbors do not change. This is consistent with the view of the formation of the cage structure due to hydrophobic hydration. By this cage structure it can also be accounted for that the peaks due to TBA-TBA interference in the 17% solution are at longer distances than the corresponding distances of pure TBA.

With an increase of the temperature, this cage structure becomes partially loose, which is pronounced in the change of the second peak (at 5.1 Å) in the distribution curve. The loosening of the cage structure and the pushing-out of water molecules may cause the growth of the cluster $(TBA)_m(H_2O)_l$, as observed by small-angle X-ray scattering experiments.

Acknowledgment. The authors thank Miss Masami Harada for her contribution to the intensity measurements of some of the present samples.

Electron Spin Resonance Spectroscopic Study of Electronic Charge Transport in an Aromatic Diamine

Richard P. Veregin* and John R. Harbour

Xerox Research Centre of Canada, 2660 Speakman Drive, Mississauga, Ontario, Canada L5K 2L1
(Received: November 14, 1989; In Final Form: March 2, 1990)

Electron spin resonance (ESR) spectra have been obtained for the radical cation of *N,N'*-diphenyl-*N,N'*-bis(3-methylphenyl)-1,1'-biphenyl-4,4'-diamine (TPD) in dichloromethane solution, in solid amorphous films, and in TPD/polycarbonate films doped with tris(*p*-bromophenyl)ammoniumyl hexachloroantimonate or HNO₃. By use of ESR the mediation of electronic charge (hole) transport via the TPD⁺ radical cation has been observed in the TPD films in the absence of an applied field. Arrhenius activation parameters were calculated for charge transport from the ESR data, giving $E_a = 10 \pm 2$ kJ/mol, $A = (1.7 \pm 1) \times 10^{10}$ s⁻¹, and a rate constant at 300 K of $(3.1 \pm 1) \times 10^8$ s⁻¹. The value of E_a is one-half that from time-of-flight (TOF) measurements extrapolated to zero field, while the rate constant is a factor of 10 smaller, and A is a factor of 1000 smaller. The differences can be understood in terms of the compensation effect due to the presence of residual solvent, and the ion pairing of an TPD⁺ ions with dopant counterions. In TPD/polycarbonate films the rate of hole transport is too slow to produce significant changes in the ESR spectrum. The rate of charge transport is thus less than 2×10^8 s⁻¹ in these films, consistent with TOF data. In dichloromethane solution, an E_a of 9.8 kJ/mol was observed with ESR. Extrapolating the solution data to solid TPD gives a hole transport rate of 9.75×10^9 s⁻¹, a factor of 3 higher than that from TOF data. The lower E_a and higher rate in dichloromethane solution are consistent with the effect of the higher dielectric constant compared to an TPD film. This suggests that the rate-determining step for hole transport is the same in solution as it is in the solid state.

Introduction

Electronic charge transport in amorphous organic materials, such as aromatic amines dispersed in inactive polymeric binders,¹⁻³ is well-known. There is general agreement that electronic charge transport in these materials is an electric field driven chain of redox processes involving neutral molecules and their charged derivatives, anion radicals for electron transport, and cation radicals for hole transport.⁴ Thus, for *N,N'*-diphenyl-*N,N'*-bis(3-methylphenyl)-1,1'-biphenyl-4,4'-diamine (TPD) the mechanism of hole transport involves a series of one-electron hopping processes whereby a neutral TPD molecule transfers an electron to a neighboring TPD cation radical, TPD⁺.¹⁻³ Measurement of the charge transport is typically done by the established time-of-flight technique. This involves photoconductivity measurements on a multilayer device such as shown in Figure 1, with a layer of semitransparent gold, over a layer containing the charge transport material and a layer of a photosensitive material such as selenium which is coated on an aluminum ground plate.¹ An applied voltage produces an electric field that causes a photogenerated hole to drift through the transport layer (TPD dispersed in a polycarbonate resin) to the negatively charged top surface where it

is neutralized. A measurement of the time for the discharge of the surface voltage after the light pulse that generates the hole enables the calculation of hole transport mobility.

The purpose of the present work is to use the TPD hole transport material to show (1) that electron spin resonance (ESR) spectroscopy can be used to directly observe hole transport, in the absence of an applied field, as it is mediated by redox processes involving intermediate cation radicals; (2) that the ESR data can be used to obtain kinetic data and activation parameters for charge transport processes; and (3) that these ESR-derived activation parameters for hole transport in TPD are consistent with those from the established time-of-flight method.

Experimental Section

Materials. *N,N'*-Diphenyl-*N,N'*-bis(3-methylphenyl)-1,1'-biphenyl-4,4'-diamine, or TPD, was obtained from Dr. Giuseppa DiPaola-Baranyi, Xerox Research Centre of Canada. The polycarbonate resin is a Bisphenol-A-polycarbonate. Tris(*p*-bromophenyl)ammoniumyl hexachloroantimonate was from Aldrich.

Sample Preparation. Films were cast from dichloromethane solutions. About 0.1 mL of solution is placed in the bottom of a quartz ESR tube, and coating is accomplished by vortexing under vacuum suction. The films are then dried under vacuum overnight at room temperature. Doping of the films with TPD⁺ cation was accomplished either by adding tris(*p*-bromophenyl)ammoniumyl hexachloroantimonate (TAH) to the casting solution, or by ex-

(1) (a) Stolka, M.; Yanus, J. F.; Pai, D. M. *J. Phys. Chem.* **1984**, *88*, 4707.
(b) Facci, J. S.; Stolka, M. *Philos. Mag. B* **1986**, *54*, 1.
(2) Pai, D. M.; Yanus, J. F.; Stolka, M. *J. Phys. Chem.* **1984**, *88*, 4714.
(3) Mort, J.; Pfister, G. *Polym.-Plast. Technol. Eng.* **1979**, *12*, 89.
(4) Bagley, D. G. *Solid State Commun.* **1970**, *8*, 345.

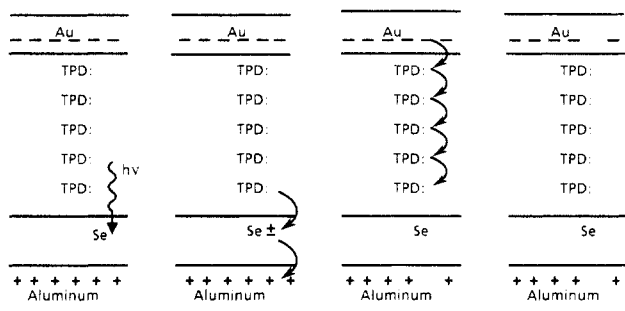


Figure 1. Model of charge transport of TPD in a device utilized in a time-of-flight measurement as described in ref 1.

posing the film to the vapor of concentrated HNO_3 for 1–2 h. Concentrations of TPD^+ were calculated from the weight of added TAH for TAH-doped samples, and by comparing the ESR signal intensity to that of a TAH-doped sample for HNO_3 -doped samples.

ESR Spectra. ESR spectra were obtained on a Varian E109E spectrometer with an E-238 TM-110 cavity, and an E-257 variable-temperature accessory, or on a Bruker ESP 300 spectrometer with a 4102 cavity, and an ER 4111 variable temperature accessory. The Mn^{2+} signal from a SrO sample was used as a reference for measurement of g values and as an internal standard for signal intensities.

Results and Discussion

Relationship between ESR and Time-of-Flight Measurements.

A simple model of the transport phenomena is that of thermally activated hopping from localized charge traps (the TPD^+ cation):⁴

$$k_h = A \exp(-E_a/kT) \quad (1)$$

Equation 1 is written in the absence of an applied field. Here k_h is the rate constant for diffusive hole transport, A is the preexponential factor (which can be seen as an attempt frequency for the thermally activated escape of the hole from the trap site), and E_a is the energy of activation that is associated with the escape of the hole from the trap. Under the influence of the field, the net hole transport diffusion can be written as⁴

$$f = f_+ - f_- = k_h \{ \exp(\rho e E / 2kT) - \exp(-\rho e E / 2kT) \} \quad (2)$$

$$\mu = \rho f / E \quad (3)$$

Here f_+ and f_- are the rates of hole transport in the direction and against the direction of the applied electric field (E), μ is the hole transport mobility (which is field dependent), and ρ is the average separation between the hopping sites (the TPD to TPD distance). Now at low field, where $\rho e E / 2kT \ll 1$, it is easy to see

$$\mu_0 = (\rho^2 e / kT) k_h \quad (4)$$

Thus the zero-field mobility, μ_0 , can be related to the rate constant for the escape from the trap site by using this model. As we shall see, ESR is sensitive to the rate of escape from the trap site and thus can be related to the mobility from the TOF measurements.

TPD in Dichloromethane. The ESR spectra of the TPD^+ radical cation in dichloromethane solution illustrate the sensitivity of ESR to molecular motion, to electron–electron exchange, and to electronic hole transport. The ESR spectrum of the TPD^+ radical cation (produced by doping with tris(*p*-bromophenyl)ammonium hexachloroantimonate, TAH) in dilute dichloromethane (8×10^{-3} M TPD, 8×10^{-4} M TPD^+) is shown in Figure 2. The spectrum was simulated as shown in Figure 2B, assuming an electron–nuclear hyperfine coupling of $a_N = 4.45$ G to two equivalent spin 1 nuclei (the two nitrogen atoms of TPD^+). The coupling to the remaining 32 protons was unresolved in the spectrum and was simulated as a Gaussian line shape of unresolved couplings with a peak-to-peak line width, $\Delta H_{pp} = 4.15$ G. The unpaired electron of the cation radical, which is associated with the “hole”, can thus be roughly viewed as having 2/3 of its electron density, ρ , in the π -system of the aromatic rings, and 1/3 of its

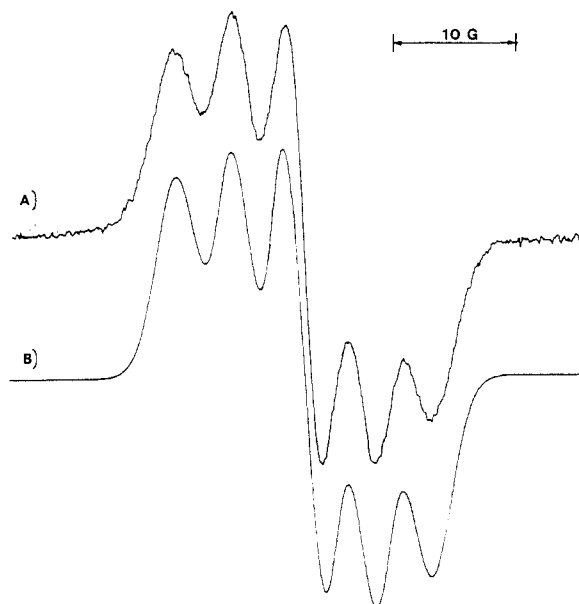


Figure 2. (A) ESR spectrum of TPD^+ in dilute dichloromethane solution at room temperature: $[\text{TPD}] = 8 \times 10^{-3}$ M, $[\text{TPD}^+] = 8 \times 10^{-4}$ M. (B) Computer simulation of ESR spectrum with hyperfine couplings to two nitrogen nuclei: $a_N = 4.45$ G, and unresolved proton couplings with Gaussian line shape of $\Delta H_{pp} = 4.15$ G.

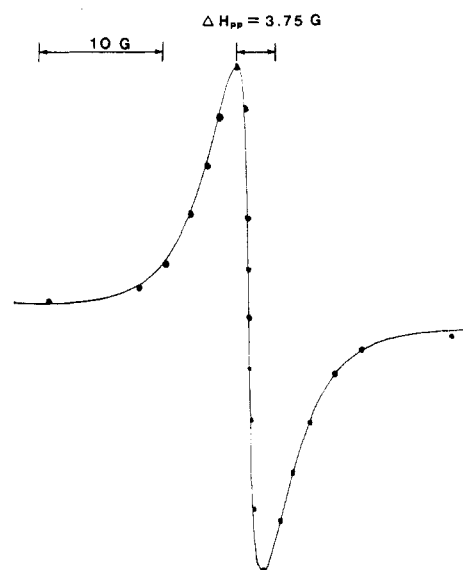
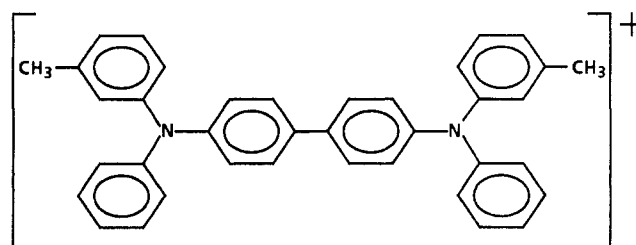


Figure 3. ESR spectrum of TPD in concentrated dichloromethane solution at room temperature: $[\text{TPD}] = 0.18$ M, $[\text{TPD}^+] = 8 \times 10^{-4}$ M. The closed circles show the fit to a Lorentzian exchange-narrowed line, with $\Delta H_{pp} = 3.75$ G.

electron density divided equally between the two nitrogen atoms, 1 (since $a_N = Q_N \rho_N$, $a_H = Q_{CH} \rho_C$, $Q_N \approx |Q_{CH}| \approx 25$ G).⁵ The



1

ESR spectrum is good evidence of an extended π -system conju-

(5) Carrington, A.; McLachlan, A. D. *Introduction to Magnetic Resonance*; Chapman and Hall: London, 1979.

gated across the biphenyl bridge and including the nitrogen lone pairs. This spectrum arises from isolated TPD molecules which are freely rotating in solution. If the TPD molecules are not isolated from each other then the ESR spectrum will change dramatically. This is shown in Figure 3 for an TPD^+ concentration that is unchanged at 8×10^{-4} M, but with a much higher concentration of TPD in dichloromethane solution. The spectrum now shows a single ESR line, with a Lorentzian line shape, which is a result of exchange which is faster than the spectral width of the ESR lines that are being averaged, $\nu_{\text{ex}} > \gamma_e \Delta\nu$. Here ν_{ex} is the rate of the exchange, $\Delta\nu$ is the largest separation of lines in the spectrum in the absence of exchange (in gauss), and γ_e is 2.8 MHz G⁻¹. The rate of exchange is thus greater than 30 MHz or 2×10^8 s⁻¹, as $\Delta\nu \sim 9$ G (i.e., $2a_N$).

There are two exchange mechanisms which could give rise to narrowing in this "fast" exchange region. One possible mechanism is the exchange interaction between two adjacent electron spins⁶ (Heisenberg exchange), as has been observed in solutions of the stable free radical 1,1'-diphenyl-2-picrylhydrazyl, DPPH.⁷ This interaction arises from the overlap of the orbitals containing unpaired electrons on adjacent TPD^+ molecules, or possibly the exchange between a TPD^+ cation and a TAH^- counterion. The rate of the exchange thus increases with $[\text{TPD}^+]$ in either case (as $[\text{TAH}^-] \approx [\text{TPD}^+]$). The other possible exchange mechanism is hole transport, which is the exchange of an electron from a neutral TPD molecule to the radical cation, with the rate of exchange now increasing with $[\text{TPD}]$. As we will show, the exchange-narrowed line width, ΔH_{pp} , of the ESR spectrum is expected to be inversely proportional to the rate of exchange. Thus the line width should narrow with increasing $[\text{TPD}^+]$ for electron-electron exchange, and with increasing $[\text{TPD}]$ for hole transport.

Piette and Anderson⁸ have calculated the effect of fast exchange on a magnetic resonance line:

$$\Delta H_{\text{pp}} - (\Delta H_{\text{pp}})_0 = (2/3^{1/2})\nabla\tau \quad (5)$$

In this case ΔH_{pp} will be the observed exchange-narrowed line width of the ESR spectrum, $(\Delta H_{\text{pp}})_0$ is ΔH_{pp} in the absence of exchange, ∇ is the second moment of the spectrum, and τ is the mean lifetime of TPD^+ . The mean lifetime is determined by the sum of the rates of all exchange processes that exchange the electron spin state of TPD^+ cation "holes":

$$1/\tau = k = k_h + k_{++} + k_{+-} \quad (6)$$

Here k_h is the rate of interchange of an electron from an TPD molecule to TPD^+ (this is hole transport as expressed in eqs 1-4), k_{++} is the rate of mutual electron spin flips, which occurs between the unpaired electrons on two TPD^+ cations, and k_{+-} is the rate of mutual electron spin flips between an TPD^+ cation and the TAH^- counterion. Equations 5 and 6 are generally true. In solution the processes of exchange will be dominated by bimolecular collisions⁹ of TPD^+ cations with TPD, TPD^+ , or TAH^- . Thus in solution

$$1/\tau = k'_h[\text{TPD}] + k'_{++}[\text{TPD}^+] + k'_{+-}[\text{TPD}^+] \quad (7)$$

The k' are the bimolecular rate constants in solution. Note that $[\text{TPD}^+]$ has replaced $[\text{TAH}^-]$, since they are proportional, with the proportionality constant (~ 1) being included in k'_{+-} . The first term of eq 7 is the term describing hole transport in solution. Combining eq 5 and 7 and defining the electron-electron exchange rate constant, $k'_{ee} = k'_{++} + k'_{+-}$ gives

$$(2/3^{1/2})\nabla\{\Delta H_{\text{pp}} - (\Delta H_{\text{pp}})_0\} = k'_h[\text{TPD}] + k'_{ee}[\text{TPD}^+] \quad (8)$$

Using the condition that $k'_{ee}[\text{TPD}^+] \ll k'_h[\text{TPD}]$, eq 8 becomes

$$\Delta H_{\text{pp}} = 2\nabla/[3^{1/2}k'_h[\text{TPD}]] + (\Delta H_{\text{pp}})_0 \quad (9)$$

To test eqs 8 and 9, the $[\text{TPD}^+]$ was varied over the range of

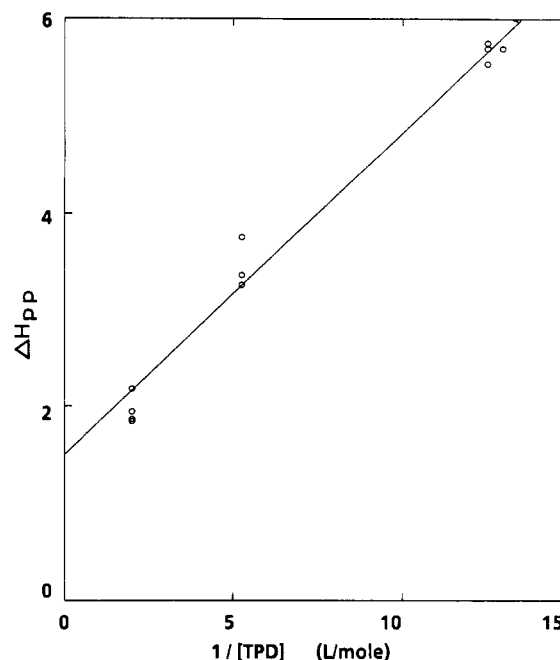


Figure 4. ESR line width as a function of $[\text{TPD}]$ in dichloromethane at room temperature. $[\text{TPD}^+] < 0.01[\text{TPD}]$. The extrapolated value of $(\Delta H_{\text{pp}})_0$ is 1.56 G.

10^{-1} – 10^{-4} M and $[\text{TPD}]$ over the range of 0 – 10^{-2} M in dichloromethane solution, resulting in observed fast-exchange-narrowed Lorentzian line widths of 2.2–7.7 G. Using the assumption that $(\Delta H_{\text{pp}})_0 \ll \Delta H_{\text{pp}}$, it was found that the data fit eq 8 quite well, with $k'_h/k'_{ee} = 3.93$ ($r = 0.96$ on 11 points). When only the data is used with $[\text{TPD}^+] < 0.01[\text{TPD}]$ and $[\text{TPD}]$ varied from 5×10^{-2} to 0.5 M, eq 9 will be valid, and $(\Delta H_{\text{pp}})_0$ can be determined. The plot of ΔH_{pp} versus $1/[\text{TPD}]$ is shown in Figure 4. The value of $(\Delta H_{\text{pp}})_0$ is 1.56 G. Using the value of 1.56 G in eq 8 yields a final corrected value of $k'_h/k'_{ee} = 3.57$ ($r = 0.97$).

To this point the temperature dependence of the exchange rate has not been considered. We can modify eq 9, by assuming that the exchange which occurs on the collision of TPD^+ with TPD (hole transport) has an activation energy, and thus $k'_h = A \exp[-E_a/RT]$, as in eq 1. Equation 9 then becomes

$$\ln \{\Delta H_{\text{pp}} - (\Delta H_{\text{pp}})_0\} = \ln \{2\nabla/(3^{1/2}A[\text{TPD}])\} + E_a/RT \quad (10)$$

Thus, from eq 10, a plot of $\ln(\Delta H_{\text{pp}} - 1.56)$ versus $1/T$ should be linear with a slope of E_a/R . This plot is shown in Figure 5 and yields $E_a = 9.8$ kJ/mol, while the Arrhenius A value is 1.85×10^{11} L mol⁻¹ s⁻¹. This activation energy is about a factor of 2 smaller than that measured in the solid state for hole transport in an TPD film by using time-of-flight measurements (20 kJ/mol).

At lower temperatures dichloromethane freezes ($T = 178$ K), and the ESR spectrum broadens dramatically to give an asymmetric resonance that is no longer exchange narrowed (and thus a resonance whose shape is no longer temperature dependent) as shown in Figure 6. Thus, in the solid the rate of the hole transport is $k_h \ll \gamma_e \Delta\nu = 25$ MHz. The spectrum in Figure 6 is thus that of TPD in the absence of exchange. The second moment of the spectrum, ∇ , can now be measured from this spectrum, or from the spectrum in Figure 2 (it is very difficult experimentally to measure the second moment of an ESR line in the presence of exchange), and is found to be 66.8 G². Using this value in eq 10, we can calculate the rate constant for the exchange any concentration, and any temperature, $k_h = k'_h[\text{TPD}]$. At 300 K the value of k'_h is 4.24×10^9 s⁻¹ L mol⁻¹. This rate constant can be extrapolated to solid TPD, i.e., $[\text{TPD}] = 2.3$ M, giving $k_h = 9.75 \times 10^9$ s⁻¹. This value of k_h is comparable to that from time-of-flight measurements, where a value of 2.87×10^9 s⁻¹ at 300 K has been measured (k is calculated from μ_0 by using eq 4). The higher value of k_h and the lower value of E_a are consistent with the higher dielectric constant of dichloromethane compared to TPD solid.¹⁰

(6) Plachy, W.; Kivelson, D. *J. Chem. Phys.* **1967**, *47*, 3312.

(7) Pake, G. E.; Tuttle, T. R., Jr. *Phys. Rev. Lett.* **1959**, *3*, 434.

(8) Piette, L. H.; Anderson, W. A. *J. Chem. Phys.* **1959**, *30*, 899.

(9) Ward, R. L.; Weissman, S. I. *J. Am. Chem. Soc.* **1957**, *79*, 2086.

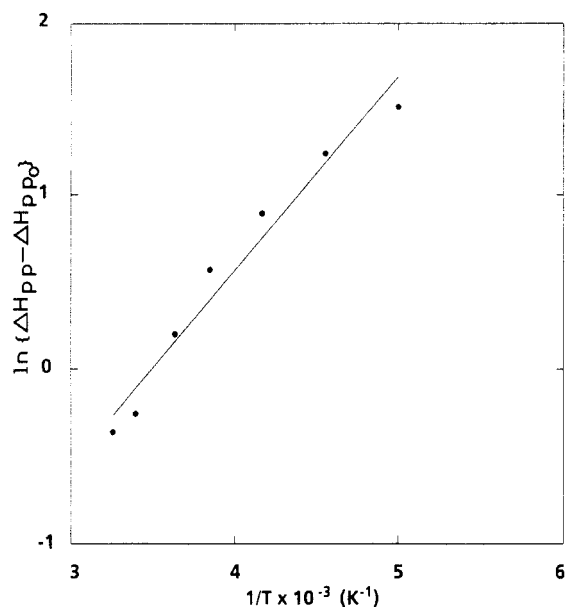


Figure 5. Plot of eq 10 for a 0.51 M solution of TPD in dichloromethane. $[\text{TPD}^+] = 0.024[\text{TPD}]$. The free energy of activation is $E_a = 9.8$ kJ/mol, from the best linear fit shown in the Figure.

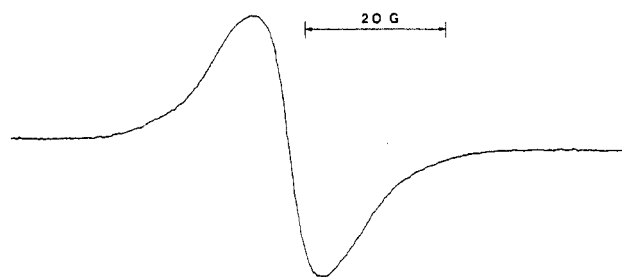


Figure 6. ESR spectrum of 0.51 M TPD in frozen solid dichloromethane at 115 K. At this temperature the rate of exchange is too slow to show any effect on this ESR spectrum.

This value of E_a is not, however, consistent with that expected for a diffusion-controlled reaction.¹¹ The activation energy in this case would be 6.9 kJ/mol, equal to the activation energy for the viscosity of dichloromethane.¹² Thus the reaction is controlled by the reorganization and exchange between a complex consisting of a radical cation and neutral molecule, rather than their diffusion-controlled collision. The general agreement of the ESR results in solution and the time-of-flight solid-state hole transport suggests that the rate-controlling step in solution is the same as that in the solid state. It should also be noted that the value of $A = 1.85 \times 10^{11}$ L mol⁻¹ s⁻¹ is consistent with the Marcus theory for solvent reorganization, which is typically 10^{11} L mol⁻¹ s⁻¹.¹³

TPD and TPD/Polycarbonate Films. The ESR spectrum at room temperature of 5% TPD⁺ (produced by doping with TAH) in a TPD film is shown in Figure 7. As in concentrated dichloromethane solution, the observed line is an exchange-narrowed Lorentzian ESR line with no observed hyperfine coupling. Again the rate of exchange must be greater than $\sim 2 \times 10^8$ s⁻¹. The ESR spectra at room temperature of $\sim 1\%$ TPD⁺ in TPD/polycarbonate films with 80%, 60%, 50%, 30%, and 20% TPD were obtained, and some of them are shown in Figure 8. Comparing the spectra in Figure 8 (as well as Figure 6, which shows the spectrum with no exchange where the matrix is frozen dichloro-

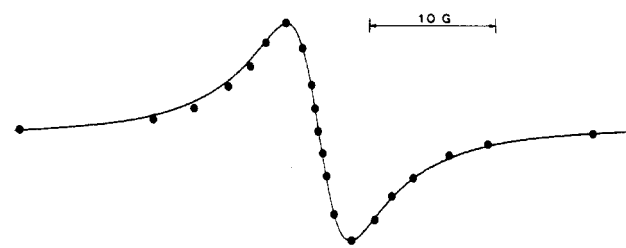


Figure 7. ESR spectrum of TPD⁺ in a dried TPD film at 130 K. The 5% TPD⁺ was produced with tris(*p*-bromophenyl)ammoniumyl hexachloroantimonate (TAH). The filled circles show the best fit to a Lorentzian "fast"-exchange-narrowed ESR line.

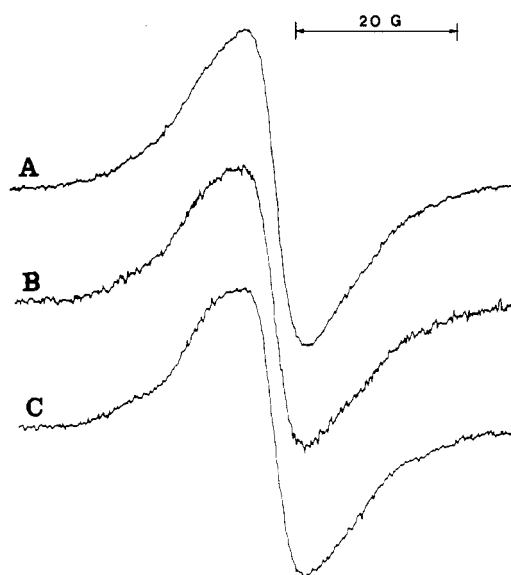


Figure 8. ESR spectrum $\sim 1\%$ TPD⁺ in a dried TPD film/polycarbonate films. The TPD⁺ was produced with tris(*p*-bromophenyl)ammoniumyl hexachloroantimonate: (A) 80% TPD; (B) 60% TPD; (C) 20% TPD. These spectra can be compared to the spectrum in Figure 6, which shows TPD⁺ with no exchange narrowing in a frozen dichloromethane matrix.

methane) shows that for all these films in polycarbonate there is very little observable exchange effect on the ESR spectrum, and thus the rate of all exchange processes must be less than 2×10^8 s⁻¹.

In the solid state we cannot write eq 7, as there is no reason to believe that either the electron-electron exchange or exchange due to hole transport can be represented by bimolecular elementary rate processes. If the exchange narrowing of the ESR resonance due to hole transport is modeled as a thermally activated release from charge traps, as shown by eq 1, then we can write

$$k_h = A \exp\{-E_a/RT\} \quad (11)$$

The electron-electron exchange rate, k_{ee} , on the other hand is expected to be independent of temperature in the solid state.¹⁴ However, it is expected to decrease rapidly as the separation of the two unpaired spins increases. For the solid state, eq 6 and 11 can be combined:

$$\ln [2\gamma / (3^{1/2} \Delta\Delta H_{pp}) - k_{ee}] = \ln A - E_a/RT \quad (12)$$

Here $\Delta\Delta H_{pp} = \Delta H_{pp} - (\Delta H_{pp})_0$. Unfortunately $(\Delta H_{pp})_0$, the line width in the absence of exchange, cannot be measured from an equation like 9 in the solid state. The alternative is to measure $(\Delta H_{pp})_0$ from the ESR spectrum of TPD⁺ which shows negligible exchange narrowing, as for a sample with low TPD concentration in a polycarbonate film. The natural line width in the absence of exchange, $(\Delta H_{pp})_0$ can then be determined from the dependence of the intensity of the ESR absorption signal, as a function of the microwave power, as shown in Figure 9 for a film with 32% TPD in polycarbonate. By use of tables for the error function,¹⁵ the

(10) Rosenberg, H.; Bhowmik, B. B.; Harder, H. C.; Postow, E. *J. Chem. Phys.* **1968**, *49*, 4108.

(11) Shimada, K.; Shimoizato, Y.; Szwarc, M. *J. Am. Chem. Soc.* **1975**, *97*, 5834.

(12) Washburn, E. W.; West, C. J.; Dorsey, W. E.; Ring, M. D., Eds., *International Critical Tables*; McGraw-Hill: New York, 1930; Vol. 7, p 213.

(13) Marcus, R. A. *J. Chem. Phys.* **1956**, *24*, 966; **1965**, *43*, 679; *Discuss. Faraday Soc.* **1960**, *29*, 21.

(14) Weiss, R. R. *Rev. Mod. Phys.* **1953**, *25*, 269.

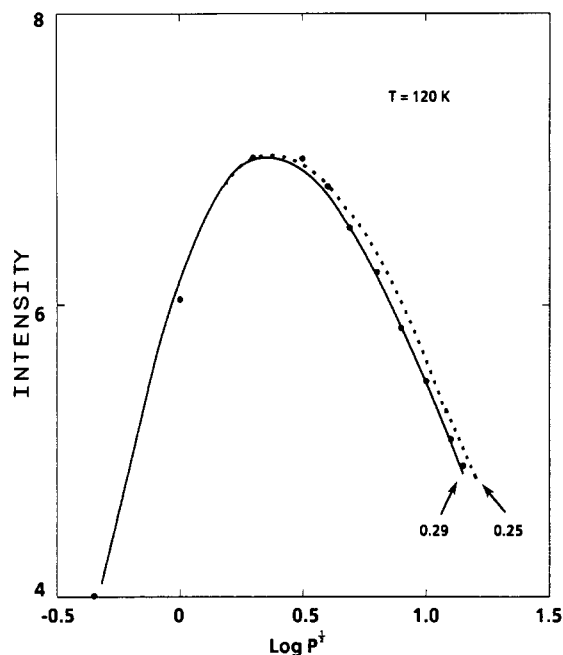


Figure 9. Microwave power dependence of the intensity of the ESR spectrum of a film of 32% TPD in polycarbonate at 120 K. The solid line and dashed line show the calculated power dependence based on two different values of $(\Delta H_{pp})_0$.

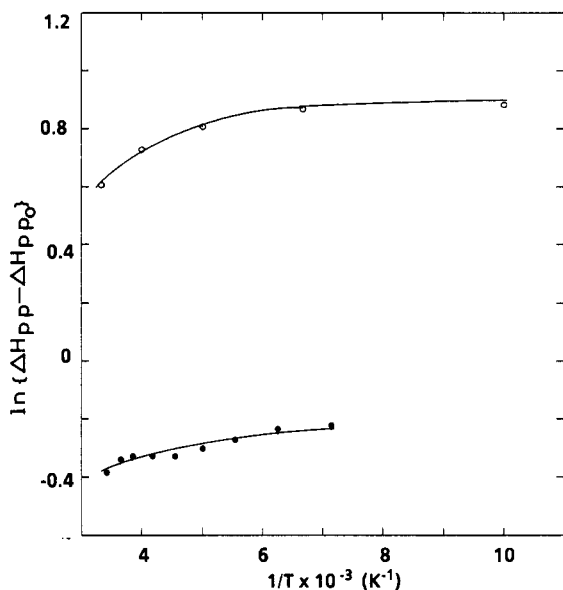


Figure 10. Temperature dependence of line width of ESR spectra of TPD films doped with TAH. The solid line shows the best fit line whose activation parameters are given in Table I: (O) 25% TPD⁺; (●) 100% TPD⁺.

power dependence curve can be calculated,¹⁶ as shown in Figure 9 for two values of $(\Delta H_{pp})_0$. In this way $(\Delta H_{pp})_0$ was calculated at 120 and 300 K to be 0.29 and 0.41 G, respectively. Values at intermediate temperatures were linearly interpolated.

The second problem with eq 12 is to find the value of k_{ee} . Clearly, if the temperature is high enough, k_{ee} is negligible, and a linear plot will be obtained if $\ln\{\Delta H_{pp} - (\Delta H_{pp})_0\}$ is plotted versus $1/T$. Using this assumption, we show a number of plots in Figure 10 with 25 and 100 wt % TPD⁺, and in Figure 11, for samples with 2 wt % TPD⁺ in solid TPD films. Clearly, at 100% TPD⁺ the exchange is dominated by electron-electron processes, giving a basically temperature-independent line width. At 2 wt %, and

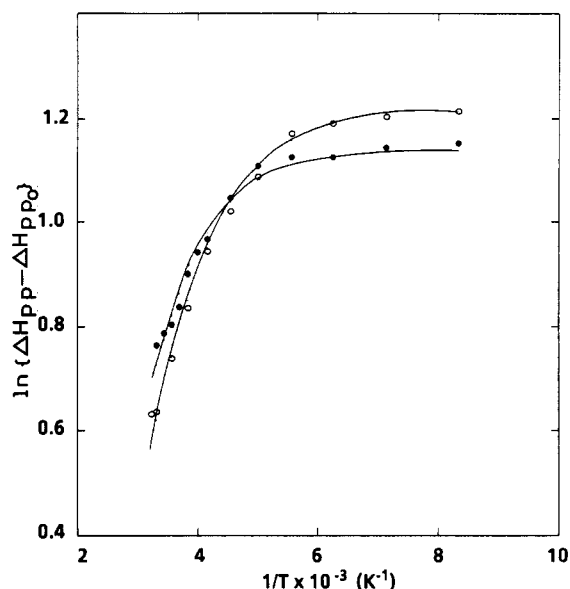


Figure 11. Temperature dependence of line width of ESR spectra of TPD films containing 2% TPD⁺. The solid line shows the best fit line whose activation parameters are given in Table I: (●) doped with TAH; (O) doped with HNO₃.

TABLE I: Hole Transport Parameters for TPD Films from ESR Data

dopant, wt %	E_a , kJ/mol	A , s ⁻¹	k_{h300} , s ⁻¹
TOF ^a	20	1.3×10^{13}	2.9×10^9
I. 0.2% TAH	9.2	1.2×10^{10}	3.2×10^8
II. 2% TAH	10.7	1.6×10^{10}	2.2×10^8
III. 2% TAH	8.3	4.1×10^9	4.2×10^8
IV. 2% HNO ₃	9.8	1.7×10^{10}	3.4×10^8
V. 5% TAH	12.1	2.9×10^{10}	2.3×10^8
VI. 10% TAH	14.5	5.4×10^{10}	1.6×10^8
VII. 25% TAH	~6	$\sim 2 \times 10^9$	1.8×10^8
VII. 100% TAH	~3	$\sim 1 \times 10^9$	3.3×10^8

^a Calculated from data in ref 1, extrapolated to zero field.

to a lesser extent, 25 wt %, higher temperatures (above 200 K) give a fairly linear region which is dominated by the temperature-dependent hole transport. From the low-temperature extreme where the exchange is temperature-independent, values of k_{ee} were calculated for each sample. Best fit curves of $\ln\{\Delta H_{pp} - (\Delta H_{pp})_0\}$ versus $1/T$ were calculated and are plotted in Figures 10 and 11. The resultant values for k_{h300} (the rate constant for hole transport at 300 K), E_a , and A are tabulated in Table I, as are TOF data from Stolka.¹

There is considerable sample to sample variation in Table I. The data at high dopant levels (25% and greater) will not be reliable and tend to give lower activation energies, preexponential factors, and rates. This is due to the fact that electron-electron exchange is very important at high TPD⁺ concentration, and thus the activation parameters become extremely sensitive to the value of k_{ee} . In addition, high dopant levels increase the separation of adjacent TPD/TPD⁺ pairs due to the dilution by the dopant and due to the decrease in the amount of neutral TPD. This will quite naturally lower the parameters A and k . In addition, the increase in dielectric constant will cause a decrease in E_a and an increase in the rate.¹⁰ Thus the value of E_a decreases, with a concomitant decrease in A , while k remains constant for the 25% and the 100% samples. The value of k_{ee} , which represents the rate of the electron-electron exchange interaction, depends on the exchange between two neighboring TPD⁺ ions, or between a TPD⁺ ion and a TAH⁻ counterion. As the [TPD⁺] and [TAH⁻] increase, it was expected that the value of k_{ee} would increase very rapidly. However, $k_{ee} = (4.4 \pm 0.8) \times 10^8$ s⁻¹ for all samples except the sample with 100% TPD⁺, which has a value of 1.66×10^9 s⁻¹. This may indicate that the interaction between an TPD⁺

(15) Abramowitz, M., Stegun, I. A., Eds. *Handbook Math. Functions*, Natl. Bur. Stand. Appl. Math. Ser. 1972, 55, 297.

(16) Castner, T. G. *Phys. Rev.* 1959, 115, 1506.

TABLE II: Hole Transport Parameters for TPD/Polycarbonate Films from ESR Data

TPD/polycarbonate film, wt % TPD	k_{h300}, s^{-1}	
	ESR	TOF ^a
80	$<2 \times 10^8$	1.7×10^8
50	$<2 \times 10^8$	1.6×10^7
30	$<2 \times 10^8$	3.1×10^5

^aCalculated from data in ref 1, extrapolated to zero field.

ion and a TAH^- counterion is the most important mechanism for electron-electron exchange, where the two oppositely charged ions form an ion pair, whose separation changes very little with increasing dopant concentration. Thus the rate of e^-e^- exchange would remain constant, except perhaps at the highest TPD^+ concentration, where $TPD^+-TPD^+ e^-e^-$ exchange becomes important as well.

Below 5% of dopant, the sensitivity of the parameters to the choice of k_{ee} is reduced, and the other sources of error become negligible. Some of the variation in these values appears to be due to the sample preparation, as considerable variation in the ESR line widths are noted even for samples with identical dopant levels. One factor which does seem to be important is the amount of residual dichloromethane in the sample, which we have observed to have some effect on the ESR spectrum, and the apparent rate of hole transport. Averaging values for samples I-VI gives $E_a = 10 \pm 2$ kJ/mol, $A = (1.7 \pm 1) \times 10^{10} s^{-1}$, and $k_{h300} = (3.1 \pm 1) \times 10^8$, with quoted errors at the 95% confidence level for the average over the five samples. The value of E_a is 1/2 of that from time-of-flight measurements, while k_{h300} is a factor of 10 smaller, and A is a factor of 1000 smaller. Two factors which may be responsible for this are the presence of residual solvent and the apparent ion-pairing of an TPD^+ ion with a dopant counterion. The significance of these differences between the ESR results and TOF results will be discussed later. The reasonable agreement between the time-of-flight and ESR results is good evidence that the TPD^+ is the species that is responsible for hole transport in TPD films. This represents a *direct* observation of the mediation of hole transport by TPD^+ .

For the ESR spectra of TPD/polycarbonate films shown in Figure 8, eq 12 is no longer applicable as the hole transport is now too slow to result in a Lorentzian exchange-narrowed line, although there are some changes in the line widths and line shapes as a function of TPD concentration and of temperature. However, it is difficult to obtain rate information from this data. It can be said that the value of k_{h300} for these samples is less than, and on the order of, the line width of the ESR spectrum, $\Delta H_{pp} \sim 8.4$ G (i.e. $\sim 2a_N$ or $\nabla^{1/2}$). Thus for these samples, $k_{h300} < 2 \times 10^8 s^{-1}$. Table II shows some values from TOF measurements, for comparison, which do indeed have rates $< 2 \times 10^8 s^{-1}$.

The Compensation Effect. It is apparent that the ESR results give lower activation energies (by a factor of 2), lower rates (by a factor of 10), and a lower A values (by a factor of 1000) than the TOF results. These results for the most part cannot be ascribed to changes in dielectric constant, ϵ , due to the presence of dopant and perhaps dichloromethane in the films used for ESR. An increase in ϵ would be expected to decrease E_a and to increase k (i.e., A would remain constant).¹⁰ Thus the extremely large changes in A are difficult to explain via this mechanism. The compensation effect for dark conductivities does predict exactly these type of changes.

For an organic semiconductor that has varying dark conductivity, σ , depending on the preparation conditions, it has been shown that there is a linear free energy relationship between the activation energy and the activation entropy. That is, as σ_0 (corresponding to A) increases, so does E_a , the activation energy for conduction (corresponding to E_a). Good examples are donor-acceptor complexes in cholesterol,¹⁰ polyene semiconductors,^{17,18} or nitro aromatic semiconductors after the absorption

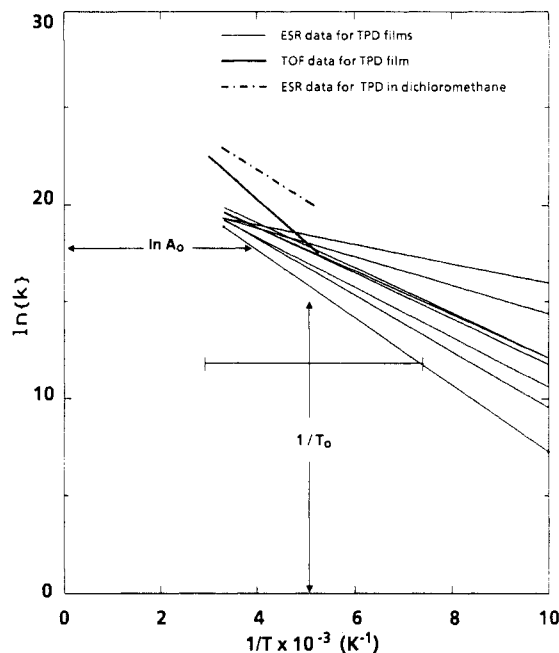


Figure 12. Plot of $\ln k_h$ versus $1/T$ showing the compensation effect. The estimated intersection point is shown as the midpoint of the range of intersections observed and gives $T_0 = 190$ K and $A_0 = 4 \times 10^7 s^{-1}$.

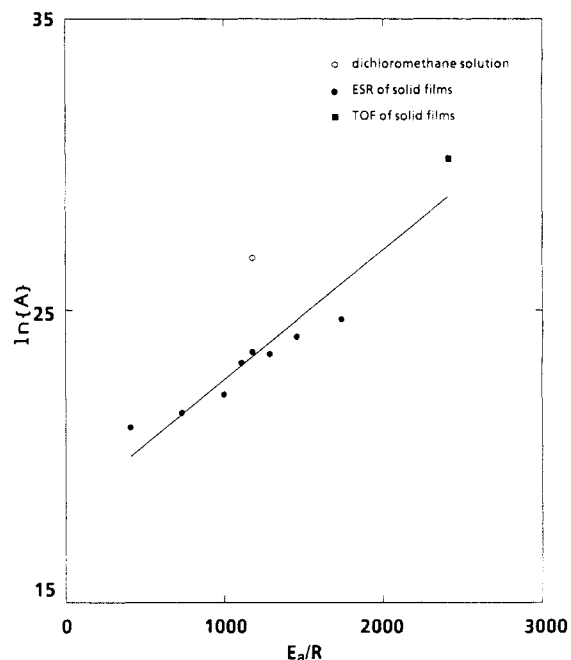


Figure 13. Plot of eq 14, $\ln A$ versus E_a/R showing the compensation effect. The slope and intercept gives $T_0 = 225$ K and $A_0 = 8 \times 10^7 s^{-1}$. The least-squares fit line shown does not include the solution data.

of organic vapors.¹⁹ We can write equations analogous to the compensation effect, since clearly the carrier mobilities are related to the conductivity. The free energy relationship can be thus defined as in eq 13:¹⁰

$$k_h = A_0 \exp\{E_a/R(1/T_0 - 1/T)\} \quad (13)$$

Here, T_0 , called the characteristic temperature and A_0 are constants. The result is that if $\ln k_h$ is plotted versus $1/T$ for each of the samples, then they will all intersect at a common point given

(18) Myachina, G. F.; Ermakova, T. G.; Lopyrev, V. A. *Phys. Status Solidi* **1984**, *81a*, 377.

(19) Gosh, A.; Jain, K. M.; Mallik, B.; Misra, T. N. *Jpn. J. Appl. Phys.* **1981**, *20*, 1059.

(17) Mallik, B.; Ghosh, A.; Misra, T. N. *Phys. Status Solidi* **1980**, *62a*, 267.

by $\ln A_0$ and $1/T_0$. By comparing eq 13, with the Arrhenius type of behavior in eq 12, we find

$$\ln A = \ln A_0 + E_a/RT_0 \quad (14)$$

Thus a plot of $\ln A$ versus E_a/R will give a straight line with intercept of $\ln A_0$ and slope of $1/T_0$. The plot of $\ln k_h$ versus $1/T$ for all the samples is shown in Figure 12. Ignoring the sample measured in dichloromethane solution, all the solid samples from ESR and TOF data intersect in the range of 150–300 K. Estimates of T_0 and A_0 are 190 K and $4 \times 10^7 \text{ s}^{-1}$, respectively. It does seem that there is another factor operating, however, which may be a contribution due to changes in the dielectric constant, in addition to a compensation effect due to the absorption of dichloromethane, and to the presence of the cation radical and its counterion. A higher dielectric constant in dichloromethane solution compared to the films would also explain the high value of $\ln k_h$ for the solution ESR data.¹⁰

Figure 13 shows the plot of eq 14 for this data, including the TOF data. The fit to eq 14 is good, with a T_0 and A_0 of 225 K and $8 \times 10^7 \text{ s}^{-1}$, in good agreement with the values from Figure 12. Again the dichloromethane data are anomalous, showing higher than expected A compared to the value of E_a , again as expected due to a change in dielectric constant. The conclusion is that the differences in k_h , A , and E_a observed within the ESR data, and in comparison with the TOF data, are due mainly to the compensation effect, with a less important effect due to changes in dielectric constant.

Conclusions

The mediation of hole-transport via the TPD⁺ radical cation has been observed directly by using electron spin resonance in TPD films. In TPD films that are doped with tris(*p*-bromophenyl)-ammoniumyl hexachloroantimonate, or HNO₃, the Arrhenius activation parameters can be calculated for hole transport from the ESR data, giving $E_a = 10 \pm 2 \text{ kJ/mol}$, $A = (1.7 \pm 1) \times 10^{10} \text{ s}^{-1}$, and $k_{h300} = (3.1 \pm 1) \times 10^8$. The value of E_a is 1/2 of that from time-of-flight measurements at zero field, while k_{h300} is a factor of 10 smaller, and A is a factor of 100 smaller. The presence of residual solvent and the ion-pairing of an TPD⁺ ion with a dopant counterion appear to be responsible for these differences. The differing results can be understood qualitatively and quantitatively in terms of the compensation effect, which has been previously applied to dark conductivity in organic semiconductors. In TPD/polycarbonate films the rate of hole transport is too low at zero field to produce significant changes in the ESR spectrum; thus the ESR results only show that the rate of hole transport must be less than $2 \times 10^{-8} \text{ s}^{-1}$ in these films. This is consistent with TOF data. In dichloromethane solution, an E_a of 9.7 kJ/mol was observed by using ESR. Extrapolating the solution data to solid TPD gave a rate of hole transport of $9.75 \times 10^9 \text{ s}^{-1}$, a factor of 3 higher than that from TOF measurements. The lower E_a and higher rate in dichloromethane solution are consistent with the effect of the higher dielectric constant compared to an TPD film. This suggests that the rate-determining step for hole transport is the same in solution as it is in the solid state.

Distance and Orientation Dependence of Electron Transfer and Exciplex Formation of Naphthyl and *p*-Dimethylanilino Groups Fixed on a Helical Polypeptide Chain

Yoshihito Inai,[†] Masahiko Sisido,^{*‡} and Yukio Imanishi[†]

Department of Polymer Chemistry, Kyoto University, Sakyo-ku, Kyoto 606, Japan, and Research Laboratory of Resources Utilization, Tokyo Institute of Technology, 4259 Nagatsuta, Midori-ku, Yokohama 227, Japan
(Received: November 15, 1989; In Final Form: March 2, 1990)

Polypeptides carrying a *p*-(dimethylamino)phenyl group (D) and a naphthyl group (N) at the middle of an α -helix chain were synthesized. The separation between D and N groups was varied by inserting different numbers (m) of alanyl units between them. The interchromophore center-to-center distance and the shortest edge-to-edge distance were estimated to be 8.3 and 5.4 ($m = 0$), 12.0 and 9.3 ($m = 1$), and 8.0 and 5.7 Å ($m = 2$). The D–N pair takes a head-to-tail orientation in the $m = 0$ polypeptide and a face-to-face orientation for the $m = 2$ polypeptide. Fluorescence from either D or N groups was markedly quenched and exciplex was formed in the $m = 0$ and 2 polypeptides, but neither quenching nor exciplex formation was observed for the $m = 1$ polypeptide. The absence of electron-transfer interactions in the $m = 1$ polypeptide indicates that the electron-transfer interactions in the polypeptides are occurring through space. The quenching efficiency was insensitive to the relative orientation of the D–N pair, but the exciplex formation was more effective in a face-to-face orientation than in a head-to-tail one. The exciplex emission of the $m = 2$ polypeptide in THF was circularly polarized ($g_{em} = 1.5 \times 10^{-3}$), indicating a specific chiral configuration of the exciplex.

Introduction

Photoexcitation of an electron donor–acceptor system leads to exciplex formation or electron transfer, depending on the nature of donor and acceptor, solvent, temperature, and other external factors.¹ Mataga and co-workers proposed that exciplex formation and electron transfer occur through different nonrelaxed charge-transfer (encounter) complexes.² However, it is still unknown what type of encounter complex leads to exciplex for-

mation and what is favorable for the electron transfer, under conditions where other external factors are kept constant. In order to answer this question, a model system in which a donor–acceptor pair is fixed with a specific distance and orientation is necessary. However, such rigid systems usually show strong ground-state interactions without forming typical exciplexes. On the other hand, a flexible system, like 3-(*p*-(dimethylamino)phenyl)propyl-1-pyrene, does not seem to form an encounter complex with a single

[†] Author to whom correspondence should be addressed at Tokyo Institute of Technology.

[†] Kyoto University.

^{*} Tokyo Institute of Technology.

(1) For a review, see, Kavarnos, G. J.; Turro, N. J. *Chem. Rev.* **1986**, *86*, 401.

(2) (a) Mataga, N. *Pure Appl. Chem.* **1984**, *56*, 1255. (b) Hirata, Y.; Kanda, Y.; Mataga, N. *J. Phys. Chem.* **1983**, *87*, 1659.